ARTICLE

Received 00th January 20xx,

Accepted 00th January 20xx

DOI: 10.1039/x0xx00000x

Room temperature synthesis of composite thin films with embedded $Cs_2AgIn_{0.9}Bi_{0.1}Cl_6$ lead-free double perovskite nanocrystals with long-term water stability, wide range pH tolerance, and high quantum yield

Steevanson Bayer, Jason Ho Yin Yu and Stefan Nagl*

Department of Chemistry, The Hong Kong University of Science and Technology

Kowloon, Hong Kong SAR, China

E-mail: chnagl@ust.hk

Supplementary information

Table of contents

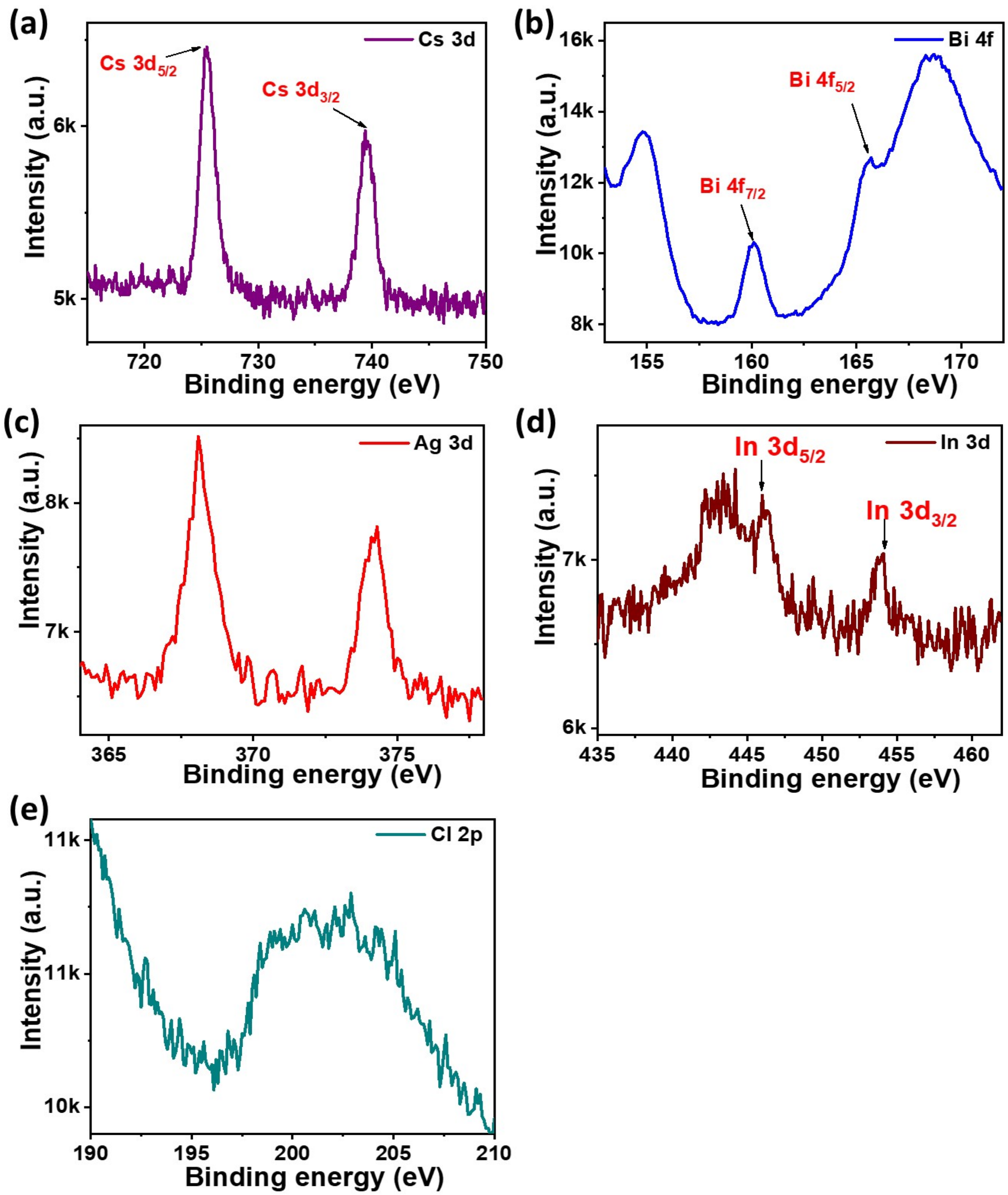

Fig. S1 XPS data of $Cs_2AgIn_{0.9}Bi_{0.1}Cl_6$ NCs confirming the constituent elements: (a) Cs 3d, (b) Bi 4f, (c) Ag 3d, (d) In 3d, (e) Cl 2p.

As shown in Fig S1 (a-d), a doublet peak was observed due to the spin-orbit coupling of the corresponding ions.

Please do not adjust margins

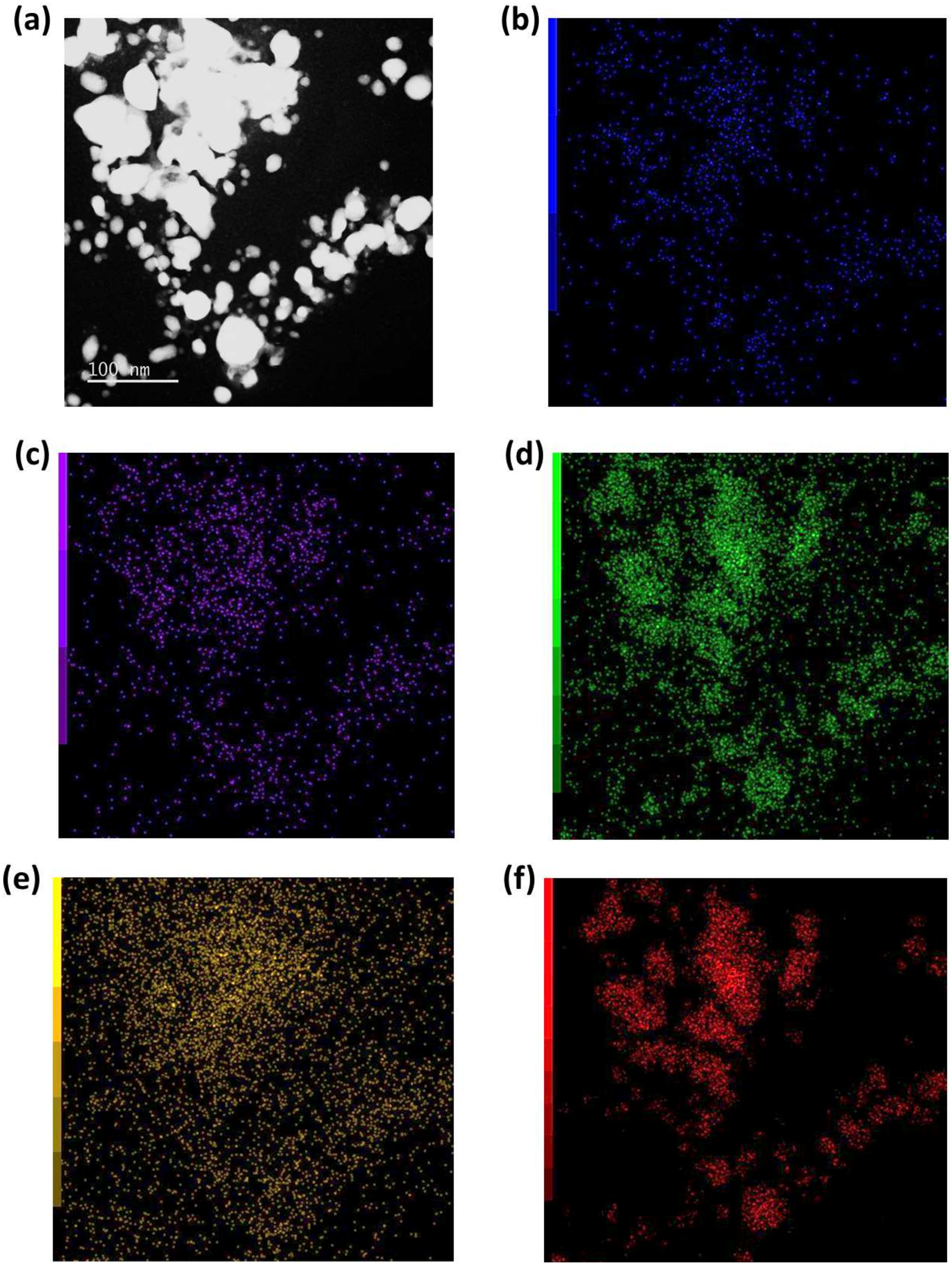

Fig. S2. EDX images of $Cs_2AgIn_{0.9}Bi_{0.1}Cl_6$ NCs showing individual elements a) HRTEM image, b) Cs, c) Bi, d) In, e) Cl, f) Ag

As shown in Fig. S2, EDX mapping of high resolution TEM images shows all the constituent elements with uniform distribution.

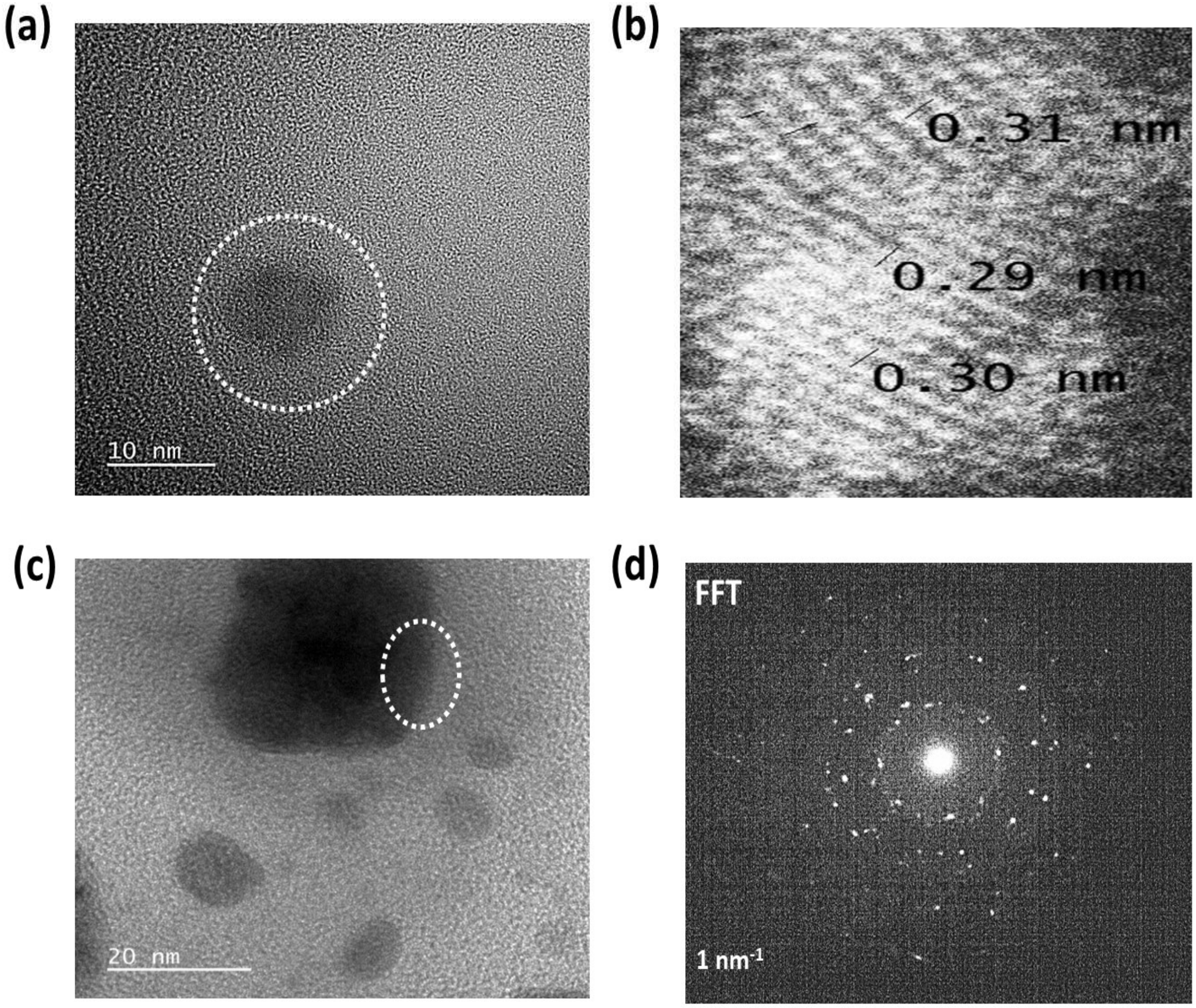

Fig. S3. HRTEM images $Cs_2AgIn_{0.9}Bi_{0.1}Cl_6$ NCs showing a) a single NC, b) shows the corresponding interplanar lattice distance for the marked area in (a), c) HRTEM image of a cluster of NCs. d) Corresponding Fast Fourier transform (FFT) pattern for the marked area in (c)

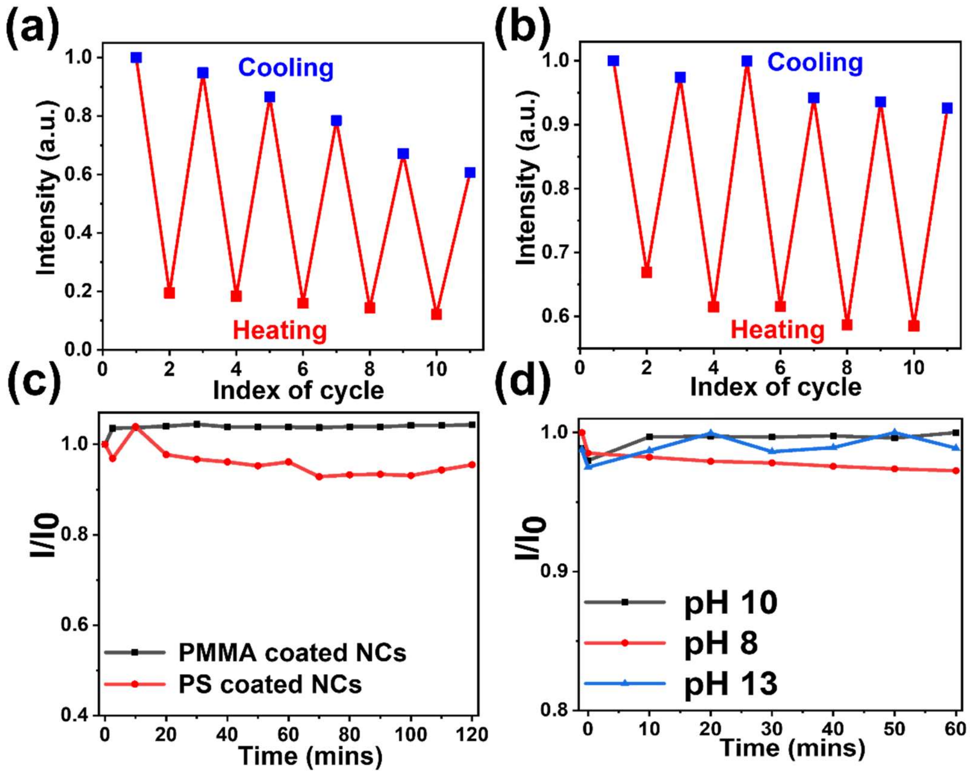

Fig. S4. a) PL intensity of PS-coated $Cs_2AgIn_{0.9}Bi_{0.1}Cl_6$ NCs and b) PL intensity of PMMA-coated $Cs_2AgIn_{0.9}Bi_{0.1}Cl_6$ NCs composite thin films over 5 consecutive heating-cooling cycles between 20 ^{0}C to 80 ^{0}C stabilized for 10 mins. c) Photostability measurements of PS and PMMA-coated $Cs_2AgIn_{0.9}Bi_{0.1}Cl_6$ thin films in contact with 100 µL water droplets for 120 mins under continuous UV irradiation. d) Photostability of PMMA $Cs_2AgIn_{0.9}Bi_{0.1}Cl_6$ thin films in contact with 100 µL BRB droplets of different pH values under continuous UV irradiation for up to 60 mins.

Thermal and photostability tests were carried out for PS and PMMA coated NCs as shown in the Fig. S4. The PMMA-coated $Cs_2AgIn_{0.9}Bi_{0.1}Cl_6$ NCs composite films showed exceptional stablity even when exposed to extremely basic conditions using BRB buffer of pH 13.

Contact angles were measured by applying a 5 µL drop of DI water on the composite thin film surface at room temperature.

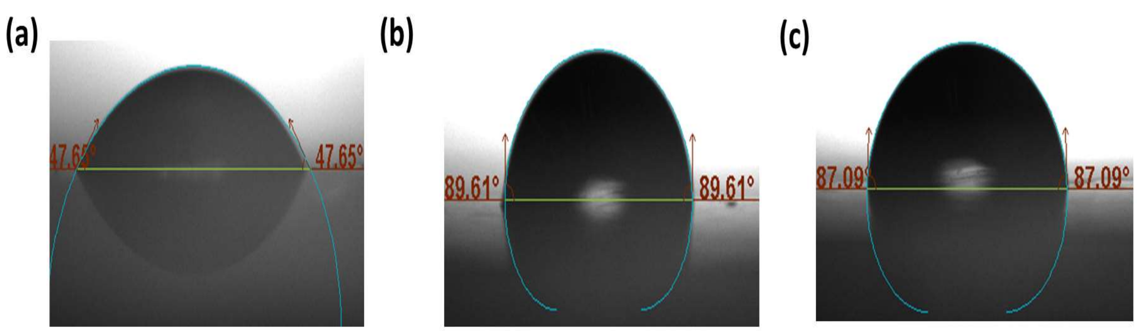

Fig. S5. Contact angles of composite thin films of $Cs_2AgIn_{0.9}Bi_{0.1}Cl_6$ NCs with a) no polymer coating, b) PS coated, and c) PMMA coated.

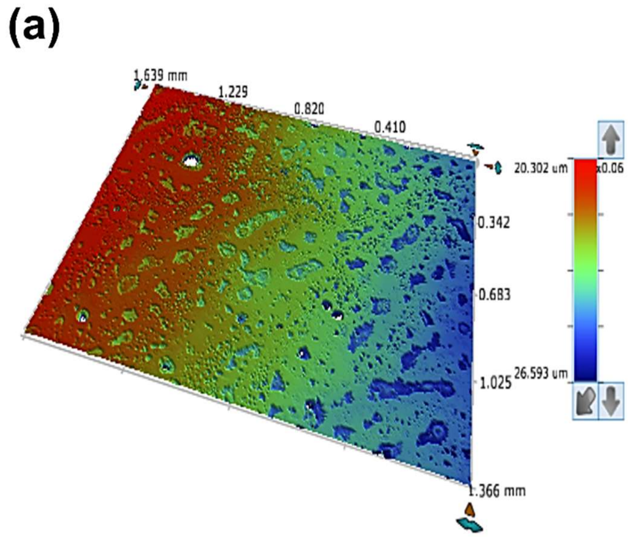

Fig. S6. Optical surface morphology of a) PS-coated $Cs_2AgIn_{0.9}Bi_{0.1}Cl_6$ NCs, b) PMMA-coated $Cs_2AgIn_{0.9}Bi_{0.1}Cl_6$ NCs.

The surface morphology of PS-coated $Cs_2AgIn_{0.9}Bi_{0.1}Cl_6$ NCs and PMMA-coated $Cs_2AgIn_{0.9}Bi_{0.1}Cl_6$ NCs was characterized by a 3D optical profiler as shown in Fig. S6. The Ra (arithmetic average roughness) and Rq (quadratic mean roughness) of PS-coated composite thin films were 8.1 µm and 9.5 µm, respectively. The Ra and Rq of PMMA-coated composite thin films were 7.5 µm and 5.7 µm, respectively.

Composition of perovskite NCs	Polymer coating/ ligands / dopants	Water stability duration	References
CH_3NH_3Br – V18	4-Vinylbenzyl-dimethyloctadecylammonium chloride (V18)	90 days	1
Cs_2SnCl_6:$_{2.75\%}$Bi	Bi	96 hrs	2
$Cs_2AgInCl_6$	None	2 days	3
$Rb_7Bi_3Cl_{16}$	None	1 month	4
$Cs_3Sb_2Br_9$	None	45 hrs	5
$Rb_{0.05}Cs_{2.95}Bi_2I_9$	None	12 hrs	6
$Cs_2Sn_{0.89}Te_{0.11}Cl_6$	Sn/Te	6 hrs	7
PEA_2SnBr_4 - g-C_3N_4	Graphitic carbon nitride (g-C_3N_4)	6 hrs	8
Cs_2ZrCl_6:Bi^{3+}	Trimethoxy(octyl)silane	1 day	9
$DMASnI_xBr_{3-x}$	CH_3-NH_2^+-CH_3	20 hrs	10
$DMASnBr_3$@g-C_3N_4	Graphitic carbon nitride (g-C_3N_4)	35 hrs	11
$CsSnCl_3$	Gelatin	3 days	12
$Cs_2Zr_{0.0021}Te_{0.0079}Cl_6$ and Cs_2ZrCl_6	$TeCl_4$ and $ZrCl_4$	10 mins	13
$Cs_3Bi_2I_9$	Polyvinylidene fluoride (PVDF)	35 days	14
$PhBz_2GeX_4$ - g-C_3N_4	Graphitic carbon nitride (g-C_3N_4)	1 day	15
$Cs_2Ag_{0.17}Na_{0.83}In_{0.88}Bi_{0.12}Cl_6$	Polyvinylidene fluoride (PVDF)	10 days	16
$(Me_3TMP)Bi_2I_9$ / $(H_3TMP)BiI_6$	1,1′,1″-(benzene-1,3,5-triyl) tris(3-methyl-1H-imidazol-3-ium)	30 days	17
$Cu_{1.4}Ag_{0.6}BiI_5$	Oleic acid / Oleylamine	7 days	18
$(H_2NDIEA)_2{\cdot}Bi_4I_{16}{\cdot}2H_2O{\cdot}4MeOH$/ $(H_2NDIEA)_2{\cdot}Bi_4I_{16}{\cdot}8H_2O$ / $[(H_2NDIEA)_2{\cdot}Bi_6I_{22}]_n{\cdot}4nH_2O$	$H_2NDIEA{\cdot}2I$	14 days	19
$Cs_2AgIn_{0.9}Bi_{0.1}Cl_6$ NCs	**Polymethylmethacrylate (PMMA)**	**4 months**	**This work**

Table S1. Comparison of water stability of lead-free perovskite nanocrystals encapsulated with different polymers or ligands reported in the literature.

As per the above comparison, the PMMA-coated $Cs_2AgIn_{0.9}Bi_{0.1}Cl_6$ NCs composite thin films exhibit superior water stability properties without using high synthesis temperature and complex surface modifications. They are low cost and provide a sustainable route for the fabrication of polymer-coated thin films.

The average PL lifetime was obtained by bi-exponential fitting of time-resolved PL traces with a $PL(t) = \Sigma_{i=1}^{n} a_i e^{-t/\tau_i}$ function

Since the PLQY is the ratio of radiative to total recombination rate, the radiative and apparent non-radiative lifetimes and rate constants can be determined as:

$$\tau_r = \frac{\langle\tau\rangle}{PLQY} \quad \text{(Suppl. Eq. 1)}$$

$$\tau_{nr} = \frac{\langle\tau\rangle}{1-PLQY} \quad \text{(Suppl. Eq. 2)}$$

$$k_r = \frac{PLQY}{\langle\tau\rangle} \quad \text{(Suppl. Eq. 3)}$$

$$k_{nr} = \frac{1}{\langle\tau\rangle} - \frac{PLQY}{\langle\tau\rangle} \quad \text{(Suppl. Eq. 4)}$$

The corresponding calculated values for all the samples are summarized below in table S2.

Properties	**As-synthesized $Cs_2AgIn_{0.9}Bi_{0.1}Cl_6$ NCs**	**PS-coated $Cs_2AgIn_{0.9}Bi_{0.1}Cl_6$ NCs**	**PMMA-coated $Cs_2AgIn_{0.9}Bi_{0.1}Cl_6$ NCs**
t_{avg}, ns	694	760	797
τ_r, ns	1943	1192	1302
τ_{nr}, ns	1081	2098	2060
k_r, ns^{-1}	514	839	768
k_{nr}, ns^{-1}	925	477	486

Table S2. Comparison of TRPL lifetime, decay rate of a) As-synthesized $Cs_2AgIn_{0.9}Bi_{0.1}Cl_6$ NCs, b) PS-coated $Cs_2AgIn_{0.9}Bi_{0.1}Cl_6$ NCs, and c) PMMA-coated $Cs_2AgIn_{0.9}Bi_{0.1}Cl_6$ NCs.

In the presence of the polymer coating, the non-radiative lifetimes increased by a factor of 2 as seen from the above table. The radiative and non-radiative rates also increase and decrease correspondingly. The decay suggests a longer lifetime for the samples with polymer coating.

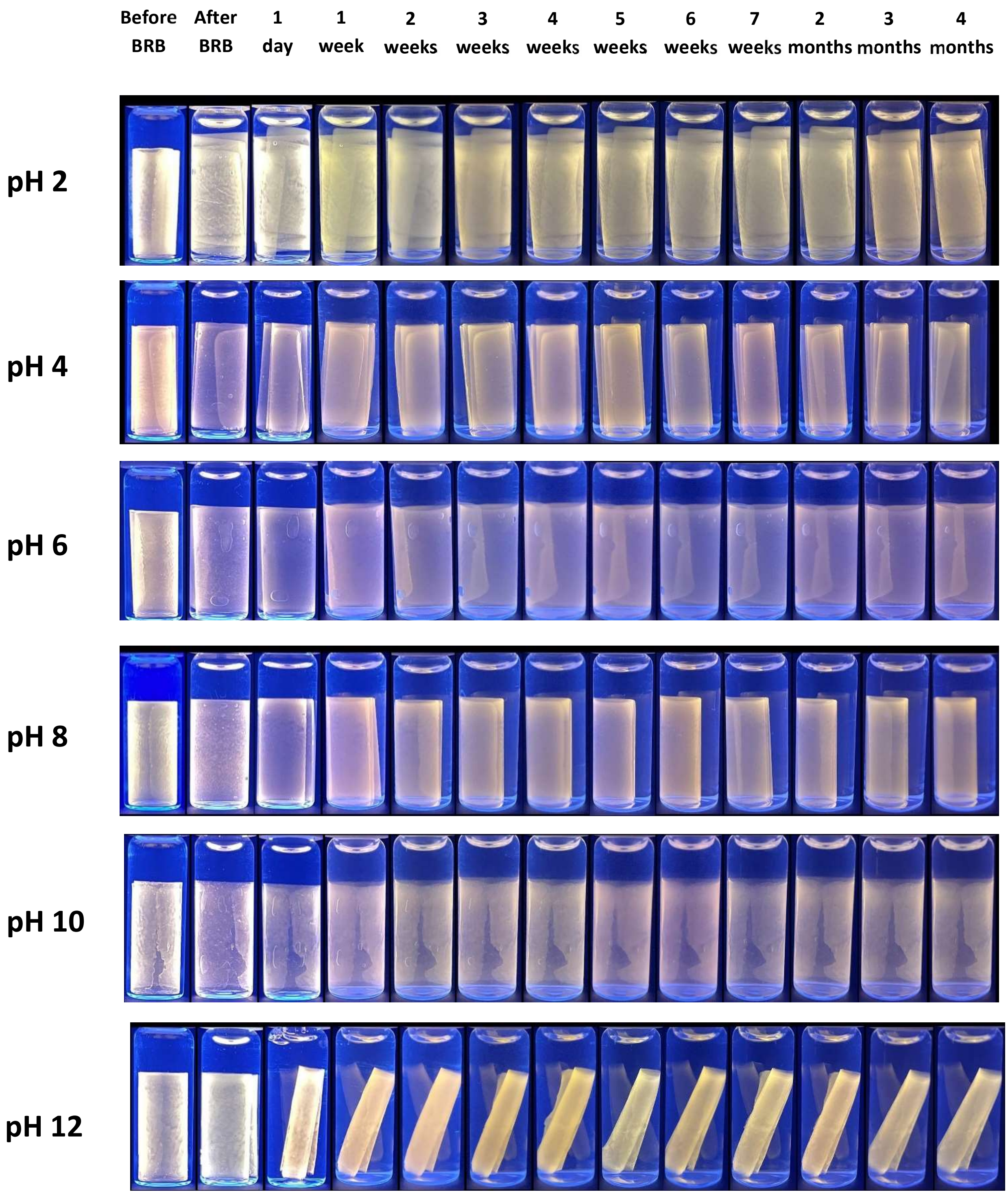

Fig. S7. Photographs of PMMA-coated $Cs_2AgIn_{0.9}Bi_{0.1}Cl_6$ thin films immersed in 4 mL BRB solution of pH 2-12 taken with a UV lamp (365 nm) at different time periods.

Supplementary References

1 H. Sun, Z. Yang, M. Wei, W. Sun, X. Li, S. Ye, Y. Zhao, H. Tan, E. L. Kynaston, T. B. Schon, H. Yan, Z. H. Lu, G. A. Ozin, E. H. Sargent, D. S. Seferos, *Adv. Mater.*, 2017, 29, 1701153.
2 Z. Tan, J. Li, C. Zhang, Z. Li, Q. Hu, Z. Xiao, T. Kamiya, H. Hosono, G. Niu, E. Lifshitz, and Y. Cheng, *Adv. Funct. Mater.*, 2018, 28 (29), 1801131.
3 W. Lee, S. Hong, and S. Kim, *J. Phys. Chem. C*, 2019, 123(4), 2665-2672.
4 L. J. Xie, Q. Z. Huang, B. Wang, J. W. Chen, X. W. Lu, X. Liu, and L. J. Song, *Nanoscale*, 2019, 11 (14), 6719-6726.
5 Z. Ma, Z. Shi, D. Yang, F. Zhang, S. Li, L. Wang, D. Wu, Y. Zhang, G. Na, L. Zhang, and X. Li, *ACS Energy Lett.*, 2019, 5(2), 385-394.
6 R. Babu, S. Bhandary, D. Chopra, and P. S. Singh, *Chem. Eur. J.*, 2020, 26 (46), 10519-10527.
7 Z. Tan, Y. Chu, J. Chen, J. Li, G. Ji, G. Niu, L. Gao, Z. Xiao, and J. Tang, *Adv. Mater.*, 2020, 32 (32), 2002443.
8 L. Romani, A. Bala, V. Kumar, A. Speltini, A. Milella, F. Fracassi, A. Listorti, A. Profumo, and L. Malavasi, *J. Mater. Chem. C*, 2020, 27, 9189-9194.
9 G. Xiong, L. Yuan, Y. Jin, H. Wu, Z. Li, B. Qu, G. Ju, L. Chen, S. Yang, and Y. Hu, *Adv. Opt. Mater.*, 2020, 8 (20), 2000779.
10 D. Ju, G. Lin, H. Xiao, Y. Zhang, S. Su, and J. Liu, *Sol RRL*, 2020, 4 (12), 2000559.
11 L. Romani, A. Speltini, F. Ambrosio, E. Mosconi, A. Profumo, M. Marelli, S. Margadonna, A. Milella, F. Fracassi, A. Listorti, F. D. Angelis, and L. Malavasi, *Angew. Chem. Int. Ed.*, 2021, 133, 3655-3662.
12 B. Lyu, X. Guo, D. Gao, M. Kou, Y. Yu, J. Ma, S. Chen, H. Wang, Y. Zhang, and X. Bao, *J. Haz. Mater.*, 2021, 403, 123967.
13 Y. Liu, Y. Wu, Z. Juan, X. Sun, W. Zhang, H. Zeng, and X. Li, *Adv. Opt. Mater.,* 2021, 9 (24), 2100815.
14 B. Mondal, H. K. Mishra, D. Sengupta, A. Kumar, A. Babu, D. Saini, V. Gupta, and D. Mandal. *Langmuir* ,2022, 40, 12157-12172.
15 L. Romani, A. Speltini, R. Chiara, M. Morana, C. Coccia, C. Tedesco, V. Armenise, S. Colella, A. Milella, A. Listorti, A. Profumo, F. Ambrosio, E. Mosconi, R. Pau, F. Pitzalis, A. Simbula, D. Ricciarelli, M. Saba, M. M. Llamas, F. D. Angelis, L. Malavasi, *Cell Rep. Phy. Sci.*, 2023, 101214.
16 J. Shi, M. Wang, C. Zhang, J. Wang, Y. Zhou, Y. Xu, and N. V. Gaponenko, *J. Mater. Chem. C*, 2023, 11, 4742-4752.
17 M. K. Li, H. Y. Lu, T. Wang, X. P. Li, N. N. Zhang, S. Q. Fan, F. Shang, N. G. Liu, and C. Li, *Inorg. Chem.*, 2023, 62 (19), 7324-7332.
18 M. Liu, K. G. Grandhi, B. Al-Anesi, H. Ali-Löytty, K. Lahtonen, R. Grisorio, and P. Vivo, *Electrochim. Acta*, 2023, 142734.
19 Q. S. Zhang, H. Fang, H. F. Chen, and J. M. Lin, *Inorg. Chem.*, 2023, 62 (48), 19706-19719.

Please do not adjust margins